of 2.37 in., inner diameter of 1.37 in., and length of 4.20 in., with ends unrestricted. The motors were conditioned to 77°F for firing, and five from a mix were fired for burning rate determination. Typical data are presented for these propellants in Fig. 1. The least squares lines were derived using de Saint Roberts burning rate law $r = aP^n$ that, although not universally true, suitably applies to these and other propellants.

The notable benefit derived from this method is typified by the lower standard deviation for r' indicated in Fig. 1. Generally, significant deviation of r from the line reflects variation in tailoff impulse. These show that r' is relatively independent of tailoff characteristics, as well as data reduction techniques for determining the aft tangent point. Therefore, Eq. (4) is likely to produce consistently a more reproducible burning rate.

A reasonable correlation was obtained between r' and full-scale motor burning rate. Typically, r' is 2–4% below corresponding full-scale motor burning rate. In particular applications, the 4 and 10% Al propellants demonstrated 2-in. r' 2 and 3% lower, respectively, than r in the full-scale motor. A burning rate of 0.749 in./sec at 1000 psia was derived from a full-scale motor firing with the mix of 8% Al propellant, in which $r' = 0.716$ in./sec. In reconciling this difference, it is recognized that average burning rate, derived by relating web to burning time and average pressure, reflects in particular the degree of augmentation from erosive burning as well as induces a slight error previously noted.[2]

References

[1] Rossini, R. A., Billheimer, J. S., and Threewit, T. R., "Configuration Efficiency: A New Measure of Ballistic Quality for Grain Design," *ARS Journal*, Vol. 31, No. 12, Dec. 1961, pp. 1761–1764.

[2] Brock, F. H., "Average Burning Rate, Average Pressure Relationships in Solid Rockets," *Journal of Spacecraft and Rockets*, Vol. 3, No. 12, Dec. 1966, pp. 1802–1803.

[3] Bartley, C. D., "Application of Simplified Method for Determining the Internal-Ballistic Characteristics of Solid Propellants," CIT/JPL-PR-20-153, Nov. 1951, Jet Propulsion Laboratory, California Institute of Technology, Pasadena, Calif.

Investigation of High Mass Ratio, Multiple-Nozzle, Air-Ejector Systems

W. A. Wright*
ARO, Inc., Tullahoma, Tenn.
AND
F. Shahrokhi†
University of Tennessee Space Institute, Tullahoma, Tenn.

LARGE, low-speed ground-testing facilities are of current interest, particularly for testing V/STOL aircraft. Motor-driven propeller systems for pumping full-scale ground test tunnels are very expensive, and elimination of this requirement in open circuit tunnels would effect considerable capital savings. One concept for this type of facility is to use a large number of air ejectors in parallel to pull air through the test section. By varying the operation of various groups of these ejectors, tunnel operation presumably could be made very flexible.

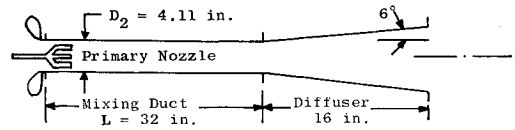

Fig. 1 Ejector configuration components, and dimensions used for the data presented herein.

There have been many studies[1–4] of jet pumps directed toward understanding of the flow phenomena and generation of a unified theory to explain the physical behavior within the flowfields. Fabri and Paulon[1] conducted an intensive investigation of the interaction between primary and secondary streams of ejector systems. Practically all of the studies considered the jet pump in the role of a pressure pumping device capable of producing a large pressure ratio from inlet to outlet under conditions favorable to this method of operation. Chisholm[5] entered the region of high secondary/primary mass flow ratios (that would be of interest here) in an investigation of thrust- and mass-augmentation using an air ejector; however, available data for high mass ratio pumping was meager. The present investigation was made to generate some data and define ejector operating characteristics in this region.

It was believed that use of multiple primary nozzles in each ejector would enhance performance and/or permit a reduction in ejector length. Therefore, data were obtained using multinozzle systems arranged in symmetric configurations intended to divide equally the mixing duct area, as well as single-nozzle configurations (Fig. 1). Secondary air at atmospheric ambient conditions was pumped through the ejector by free turbulent mixing with the higher energy driving jets in a momentum exchange process with the near-ambient total-temperature primary air taken from a shop air line. Primary driving air total pressure was varied systematically over a pressure ratio range (primary/secondary) from 1.9/1 to 8/1. Area ratios (secondary/primary) ranged from approximately 80/1 to 650/1. The mixed stream was discharged to the atmosphere in all cases.

The basic equations employed in the analysis were derived using the von Kármán integral method, wherein the stream velocity profile is prescribed. Mixing of the primary and secondary streams was assumed to occur according to the Prandtl theories concerning mixing length for turbulent shear and the eddy viscosity model, following Peters's[6,7] theoretical development. The modified analysis included a wall correction for boundary-layer displacement thickness δ^* by applying a factor to the duct wall radius as follows: $r_w = C_1 + C_2x$, where C_2 represents the displacement thickness $(-d\delta^*/dx)$. This analysis considered the back-pressure-dependent mode of operation, wherein the back pressure P_b was always high enough to preserve subsonic secondary flow throughout the length of the ejector, and the exit pressure was identical to the back pressure. Geometric "equivalency" factors were applied to the multinozzle configurations on the basis of equal

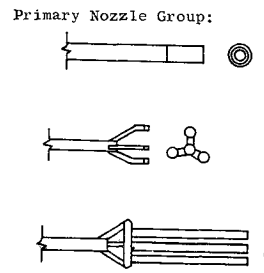

	$(L/D)_{eq}$	Total A_p^*, in.^{2}	Figs.
Type I (1 Noz.)	7.8	0.0774	3,5
Type II (3 Noz.)	4.5	0.0693 0.0202	3,5 4
Type III (7 Noz.)	2.9	0.0653	3,5

Fig. 2 Details of ejector inlet and primary nozzle configurations used for data reported herein.

Presented as Paper 70-579 at the AIAA 5th Aerodynamic Testing Conference, Tullahoma, Tenn., May 18–20, 1970; submitted May 25, 1970; revision received August 13, 1970. The research herein was sponsored by Headquarters AEDC, Arnold Air Force Station, Tenn., Contract AF 40(600)-1200 with ARO, Inc.

* Project Engineer.

† Associate Professor. Associate Fellow AIAA.

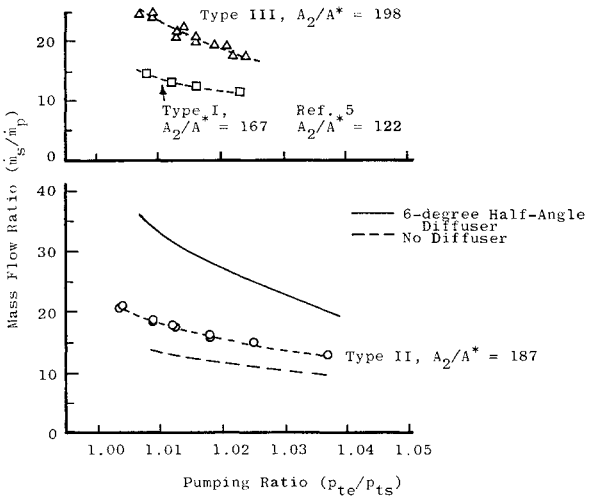

Fig. 3 Ejector performance (mass ratio vs pumping ratio).

flow areas assigned to each of n primary nozzles; i.e.,

$$D_{eq} = n^{1/2}D \qquad (L/D)_{eq} = n^{1/2}L/D$$

where D and L are duct diameter and length, respectively,

$$C_{2eq} = n^{1/2}(-d\delta^*/dx)$$

Details of the ejector (secondary air) inlet and the primary air nozzles are shown in Fig. 2. The primary nozzle flows were underexpanded in all tests. Primary and secondary air temperatures and pressures were measured, as well as static and total pressures at several stations along the ejector device. Mixing duct lengths of 16 to 36 with a 4-in. ejector, and 16 to 26 in. with a 2-in. ejector, were tested, thus included the range from 4 to 13, but only the configurations indicated in Fig. 2 are considered herein. For the data presented herein, the conical diffuser wall half-angle was 6°. The following results are typical of the better results obtained in this investigation.

Experimental Results and Conclusions

Relationships between secondary/primary mass flow ($\dot{m}_s/\dot{m}p$) and pressure pumping ratio for the three configurations of Fig. 2 are shown in Fig. 3. The pumping ratio was defined as the ratio of the inlet secondary flow total pressure to the exit flow total pressure. A small improvement in experimental performance is noted proceeding from the single central nozzle (type I) to the 7-nozzle (type III) system.

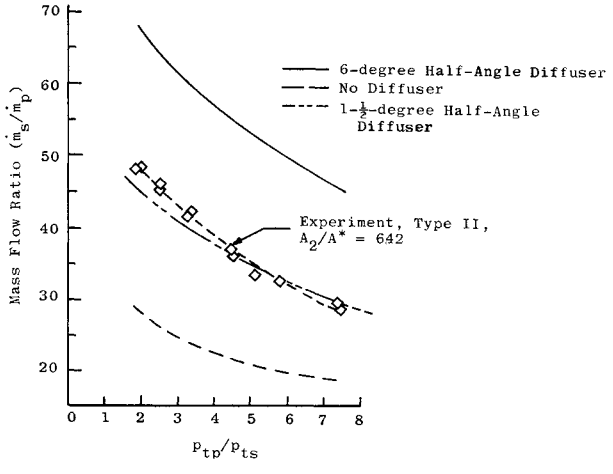

Fig. 4 Typical ejector performance (mass ratio vs stream pressure ratio).

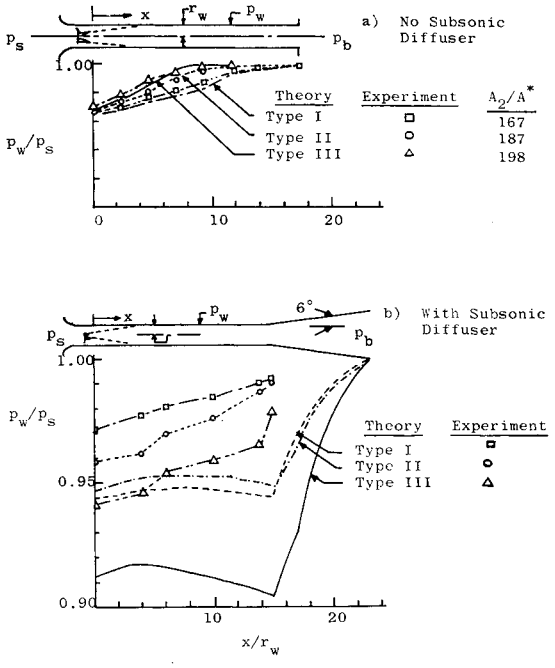

Fig. 5 Typical wall pressure profiles.

The relationship between achieved and theoretical results shown for type II was typical. A similar test result was obtained in Ref. 5 for a single central nozzle ejector at the no-load back-pressure condition, which was atmospheric pressure.

Although high mass flow ratio (35:1) pumping was obtained, p_{te}/p_{ts} was extremely low at this condition (1.003). Translating this result into performance level for an ejector-driven test tunnel using an air supply of 600 lb_m/sec at 65 psia indicates that a very large cross section (>10,000 ft²) could be driven at a tunnel velocity of 20 fps, at atmospheric inlet conditions, provided there are no losses. Results at the lowest mass flow ratio of these experiments (10:1), were $p_{te}/p_{ts} \sim 350$ ft² could be driven at 250 ft/sec.

Performance in terms of primary/secondary total pressure ratio is shown in Fig. 4. The experimental results obtained with a 6°-half-angle subsonic diffuser were comparable to the theoretical predictions for a 1.5°-half-angle diffuser. Experimental performance was low by a factor of two when compared to the fully mixed, one-dimensional analysis.

Mixing duct wall pressure profiles are shown in Fig. 5. With no subsonic diffuser installed, the duct mixing theory and the experimental results agreed closely. When a 6°-half-angle diffuser was installed, the experimental performance deviated significantly from that predicted; for each primary nozzle configuration, some type of flow separation occurred in the diffuser.

In this investigation, tests were made to optimize the number or the arrangement of the primary nozzles, and no attempt was made to solve the separation problem. It should be noted, however, that others are presently working to overcome this same difficulty in connection with high lift jet devices in the vertical take-off aircraft field.

References

[1] Fabri, J. and Paulon, J., "Theory and Experiments on Supersonic Air-to-Air Ejectors," TM 1410, Sept. 1958, NACA, Washington, D.C.

[2] Dehaan, R. E., "Supersonic Ejectors with Mixing at Constant Cross Section," *Applied Scientific Research*, Vol. 14, 1964–65, pp. 57–76.

[3] Chow, W. L. and Addy, A. L., "Interaction between Primary and Secondary Streams of Supersonic Ejector Systems and Their Performance Characteristics," *AIAA Journal*, Vol. 2, No. 4, April 1964, pp. 686–695.

[4] Donaldson, C. duP. and Gray, K. E., "Theoretical and Experimental Investigation of the Compressible Free Mixing of Two Dissimilar Gases," *AIAA Journal*, Vol. 4, No. 11, Nov. 1966, pp. 2017–2025.

[5] Chisholm, R. G. A., "Design of an Air Ejector to Operate Against Various Back Pressures," TN 39, Sept. 1960, University of Toronto, Institute of Aerophysics, Toronto, Ontario, Canada.

[6] Peters, C. E., "Turbulent Mixing and Burning of Coaxial Streams Inside a Duct of Arbitrary Shape," TR 68-270, Dec. 1968, Arnold Engineering Development Center, Arnold Air Force Station, Tenn.

[7] Peters, C. E., Phares, W. J., and Cunningham, T. H. M., "Theoretical and Experimental Studies of Ducted Mixing and Burning of Coaxial Streams," *Journal of Spacecraft and Rockets*, Vol. 6, No. 12, Dec. 1969, pp. 1435–1441.

Inaccuracy of Nozzle Performance Predictions Resulting from the Use of an Invalid Drag Law

C. T. Crowe*
Washington State University, Pullman, Wash.

ESSENTIAL to the analysis of gas-particle flow in a rocket nozzle and prediction of performance inefficiency due to the particles' thermal and velocity lags is information on the particle drag coefficient. Studies have shown[1,2] that the flow region encountered by a particle in a rocket nozzle lies within Reynolds numbers less than 10 and Mach numbers less than unity and encompasses the entire gamut of flow regimes from continuum to free-molecule flow. Until now no information has been available for the particle drag coefficient in this region and several different drag laws have been devised and utilized for nozzle-flow analyses and performance predictions. Drag coefficient data have now become available,[3] however, and the adequacy of the various drag laws can be assessed. This Note illustrates the errors in nozzle performance predictions which result from using the devised drag laws and shows the significance of the drag law in nozzle performance predictions.

A survey by Miller and Barrington[4] on the performance prediction of solid propellant rocket motors revealed that four different expressions for the particle drag coefficient have been used in the analyses of gas-particle flows in rocket nozzles. In the earlier works[5] the classical drag coefficient for a sphere in incompressible flow was employed. The discovery that the particles were not in continuum flow for the greater part of their trajectory through the nozzle led to the invention and use of three different drag laws designed to account for rarefaction effects. Kliegel[6] employed a theoretical equation which derives from a solution of the Thirteen Moment equations, namely,

$$C_D = C_{D_0}\left[\frac{(1 + 7.5Kn)(1 + 2Kn) + 1.91Kn^2}{(1 + 7.5Kn)(1 + 3Kn) + (2.29 + 5.16Kn)Kn^2}\right] \quad (1)$$

where C_{D_0} is the drag coefficient for a sphere in incompressible flow and Kn is the Knudsen number. Carlson and Hogland,[2] combining rarefaction effects measured by Millikan[7] and Reynolds number trends in incompressible flow, developed the following expression

$$C_D = \frac{24}{Re} \times \left[\frac{(1 + 0.15Re^{.687})\{1 + \exp[(0.427/M^{4.63}) - (3/Re^{0.88})]\}}{1 + (M/Re)[3.82 + 1.28\exp(-1.25\,Re/M)]}\right] \quad (2)$$

where Re and M are the particle Reynolds number and Mach number, respectively. Fitting available data at high and low Mach numbers with reasonable trends between, Crowe[8] devised the following drag law

$$C_D = (C_{D_0} - 2)\exp\left[-3.07\gamma^{1/2}\frac{M}{Re}g(Re)\right] + \frac{h(M)}{\gamma^{1/2}M}\exp\left(\frac{-Re}{2M}\right) + 2 \quad (3)$$

where

$$\log_{10} g(Re) = 1.25[1 + \tanh(0.77\log_{10} Re - 1.92)]$$

and

$$h(M) = [2.3 + 1.7(T_p/T_g)^{1/2}] - 2.3\tanh(1.17\log_{10}M)$$

with T_p and T_g being the particle and gas temperatures, respectively. Because of the absence of drag data in flow regimes encountered in a rocket nozzle, it was not possible to decide which of the preceding laws was most valid.

The problem of the particle drag coefficient in a rocket nozzle has now been resolved by data[3] taken with a microballistic range. These data were reduced in terms of a normalized coefficient suggested by Sherman,[9]

$$\bar{C}_D = (C_D - C_{D_I})/(C_{D_{FM}} - C_{D_I}) \quad (4)$$

where C_{D_I} is referred to as the "inviscid" drag coefficient, taken from high Reynolds-number data for spheres, and $C_{D_{FM}}$ is the drag coefficient for a sphere in free molecule flow.[10] The data from the microballistic range, together with other published data, were plotted vs Knudsen number and an empirical equation was developed to fit the data.

The adequacy of the devised drag laws to represent the data[3] is illustrated in Fig. 1. The expressions used by Kliegel and Carlson represent the data reasonably well at the smaller Knudsen numbers but diverge significantly from the data in the near- and free-molecule flow regimes. The expression proposed by Crowe shows better agreement but exhibits an inflection which is neither observed in the data nor predicted by theory.[11] Based on the data in Fig. 1 and other published data extending down to a Knudsen number of 10^{-3}, the fol-

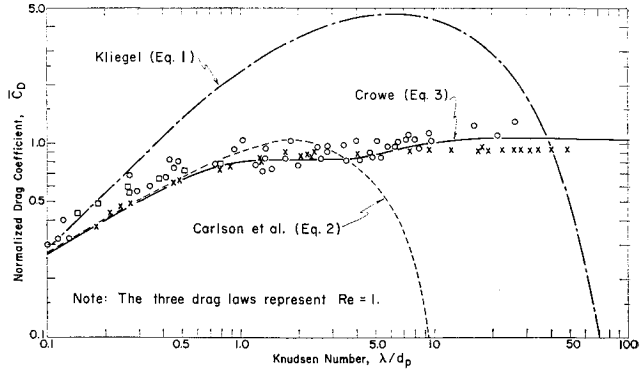

Fig. 1 Adequacy of the devised drag laws to represent data for the particle drag coefficient in flow regimes encountered in a rocket nozzle.

Received September 1, 1970. This investigation was supported in part by funds provided by the Graduate School Development Funds.

* Associate Professor, Mechanical Engineering. Member AIAA.